Molecular Crystals and Liquid Crystals

ISSN: 1542-1406 (Print) 1563-5287 (Online) Journal homepage: http://www.tandfonline.com/loi/gmcl20

Dielectric Multilayer Including Azobenzene Polymer Liquid Crystal with Non-quarter-wave Stack

Ryotaro Ozaki, Kazunori Kadowaki, Takashi Hagio, Ryohei Yagi, Yutaka Kuwahara & Seiji Kurihara

To cite this article: Ryotaro Ozaki, Kazunori Kadowaki, Takashi Hagio, Ryohei Yagi, Yutaka Kuwahara & Seiji Kurihara (2015) Dielectric Multilayer Including Azobenzene Polymer Liquid Crystal with Non-quarter-wave Stack, Molecular Crystals and Liquid Crystals, 611:1, 1-13, DOI: 10.1080/15421406.2015.1027989

To link to this article: http://dx.doi.org/10.1080/15421406.2015.1027989

Published online: 06 Jul 2015.

Mol. Cryst. and Liq. Cryst., Vol. 611: pp. 1–13, 2015

ISSN: 1542-1406 print/1563-5287 online
DOI: 10.1080/15421406.2015.1027989

Dielectric Multilayer Including Azobenzene Polymer Liquid Crystal with Non-quarter-wave Stack

RYOTARO OZAKI,[1,*] KAZUNORI KADOWAKI,[1] TAKASHI HAGIO,[2] RYOHEI YAGI,[2] YUTAKA KUWAHARA,[2] AND SEIJI KURIHARA[2,3,4]

[1]Graduate School of Science and Engineering, Ehime University, Bunkyo-cho, Matsuyama, Ehime, Japan
[2]Graduate School of Science and Technology, Kumamoto University, Kurokami, Kumamoto, Japan
[3]Kumamoto Institute for Photo-Electro Organics (PHOENICS), Higashimachi, Higashi-ku, Kumamoto, Japan
[4]JST, CREST7, Gobancho, Chiyoda-ku, Tokyo, Japan

Dielectric multilayer including azobenzene polymer liquid crystal acts as a one-dimensional photonic crystal and has optical-switchable reflection bands. The reflection intensity can be controlled by irradiation of ultraviolet (UV) or visible light, in which the optical switch is based on cis-trans photoisomerization. An increase in the number of layers prevents photoresponse in the multilayer including azobenzen layers because UV or visible light for control cis-trans isomerization hardly reach the bottom of the multilayer due to exponential decay of light intensity. In this study, the multilayer consisting of thin azobenzene layers is investigated. According to numerical calculations, the non-quarter-wave structured multilayer has multiwavelength reflection band. Angular dependence of reflection color from multiwavelength stopband is also studied using the XYZ color space. The non-quarter-wave multilayer suppresses reflection color change compared with conventional quarter-wave multilayer.

Keywords Azobenzene; polymer liquid crystal; dielectric multilayer; photonic crystal; reflection

Introduction

Liquid crystals are rod-like or disk-like organic molecules which normally have self-assembled characteristics. Owing to their molecular shape, liquid crystals have various anisotropies, such as permittivity, refractive index, and viscosity. Similarly, in polymer liquid crystals, the molecular orientation of mesogenic groups influences their physical properties such as optical, electrical, and mechanical properties [1–5]. The molecular

*Address correspondence to Ryotaro Ozaki, Graduate School of Science and Engineering, Ehime University, 3 Bunkyo-cho, Matsuyama, Ehime, 790-8577, Japan. E-mail:ozaki.ryotaro.mx@ehime-u.ac.jp

Color versions of one or more of the figures in the article can be found online at www.tandfonline.com/gmcl.

orientation of low molecular weight liquid crystals can be easily controlled by magnetic field, electric field, mechanical stress, or temperature, whereas it is generally not easy to control the molecular orientation of polymer liquid crystals mainly because of their high viscosity. There are some reports on polymers showing out-of-plane molecular orientation by annealing: side-chain type polymer liquid crystals, main-chain type polymer liquids, and so on [6–13]. However, azobenzene polymer liquid crystals can reratively easily control their mesogenic orientation using cis-trans photoisomerization. Macroscopically, the cis-trans isomerization of azobenzenes induces a change in refractive index or photo-mechanical effects [1–5]. The refractive index tunability has been utilized for dielectric multilayers [5] and opal photonic crystals [3,4]. Such optical devices are known as tunable photonic crystals which have variable photonic bandgaps by controlling optical periodicities and are also expected for functional applications, for example, tunable optical waveguides and tunable lasers [14–17]. We proposed an azobenzene polymer liquid crystal / polyvinyl alcohol (PVA) multilayer as a tunable one-dimensional photonic crystal in which switching of photonic band gap was demonstrated by ultraviolet (UV) and visible light irradiations [5].

Compared with inorganic multilayer, polymer dielectric multilayers have advantages in terms of fabrication, weight, flexibility, cost, and so on [18,19]. The polymer multilayers can be easily obtained by spin coating and it is easy to produce a large-area thin film. Lightness and scratch resistant are also advantage of the polymer multilayers compared to conventional inorganic multilayers. However, it is difficult for polymer multilayers to achieve a large refractive index contrast due to the limit of material's properties. Since the reflection bandwidth strongly depends on index contrast, the bandwidth of a polymer multilayer is generally narrower than that of inorganic one. Stacking different thickness layers is one of the solutions to the problem. A multilayer with many layers of different thicknesses can produce broadband reflection in which the thickness of layer gradually increases or decreases. The broadband reflection results low directional dependence because the wide range of wavelengths is reflected. However, an increase in the number of layers prevents photoresponse in the multilayer including azobenzen layers (azo-layers) because UV or visible light for control cis-trans isomerization hardly reach the bottom of the multilayer due to exponential decay of light intensity. Since the photoresponse in the azobenzen multilayer (azo-multilayer) is based on light absorption and cis-trans isomerization, it is an inevitable problem for the azo-multilayer. Therefore, determining a suitable multilayered structure is important for azobenzene liquid crystal polymer to achieve reflection with a low directional dependence. Here we study a non-quarter-wave multilayered structure including thin azo-layers which shows multi-peak reflections. From the reproduction of the spectral color of the multi-peak reflection, we also investigate incident angle dependence of the reflection color.

Experimental Study of Non-Quarter-Wave Stacked Multilayer Including Thin Azo-Layers

The dielectric multilayer studied here is that the azobenzene and other non-photoresponsive polymers are alternately stacked as illustrated in Fig. 1. In this study, side-chain type liquid crystal polymer Poly(6-(4-methoxy-4′-hydroxy- azobenzene)alkylacrylate) (PMAz6Ac) was used. The azobenzene polymer PMAz6Ac was synthesized by a method similar to the synthetic route reported earlier [20]. The molecular structure is shown in Figure 1(c), and the azobenzene is illustrated as rod-like molecules in Fig. 1(a) and 1(b). We have typically used PVA as the non-photoresponsive polymer layer (non-azo-layer)

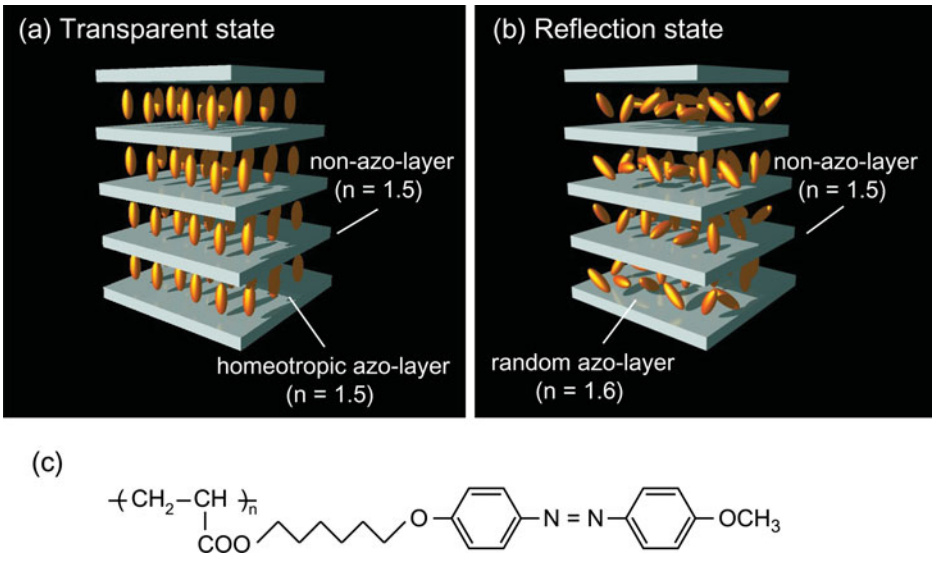

Figure 1. Schematic views of dielectric multilayers having azobenzene layers of (a) homeotropic alignment and (b) random alignment. (c) Molecular structure of poly(6-(4-methoxy-4′-hydroxy-azobenzene)alkylacrylate) (PMAz6Ac).

for fabrication of the multilayer because the refractive index of PVA is approximately the same as the ordinary refractive index of the PMAz6Ac. Therefore, when azobenzene align homeotropically, the azo-multilayer does not show strong reflection and is in transparent state as shown in Fig. 1(a). On the other hand, the bent cis-form produces a disorder in the liquid-crystalline phase, and then the molecular orientation becomes random as illustrated in Fig. 1(b). Under the condition, the multilayer show strong Bragg reflection and is in reflection state. The random orientation owing to trans-cis isomerization can be easily obtained by irradiation of UV light, and the homeotropic alignment can be obtained by irradiation of visible blue light. By the irradiation of UV or visible light, the azo-multilayer acts as optical switchable dielectric mirror.

However, as mentioned above, the strong absorption of the azobenzene does not allow switching of the reflection characteristics in a RGB-stacked multilayer which has many layers with different thicknesses. In a multilayer having thick azo-layers, UV or visible light for control molecular alignment does not reach the bottom of the multilayer. The response of the photoisomerization will be very slow because the light intensity becomes weaker at the bottom of the multilayer. To seek possibilities for a multi-stopband structure except for RGB-stacked or chirped multilayer, numerical calculations were performed using the 4×4 matrix method [21].

Figure 2 shows the calculated reflection spectra of the azo-multilayer for several optical thickness ratios of azo-layer and non-azo-layer. In these calculations, we assumed randomly oriented azobenzene molecules, and the refractive indices of the azo-layer and non-azo-layer were set to be 1.6 and 1.5, respectively. The thickness of the azo-layer was constant 80 nm, and the thickness of the non-azo-layer increased up to 19 times of the azo-layer in optical length. The number of periods was 20 for all calculations. The spectrum in Fig. 2(a) represents the reflection from a quarter-wave multilayer because the optical lengths of the azo-layer and non-azo-layer are same. There is a single reflection peak of the stopband at

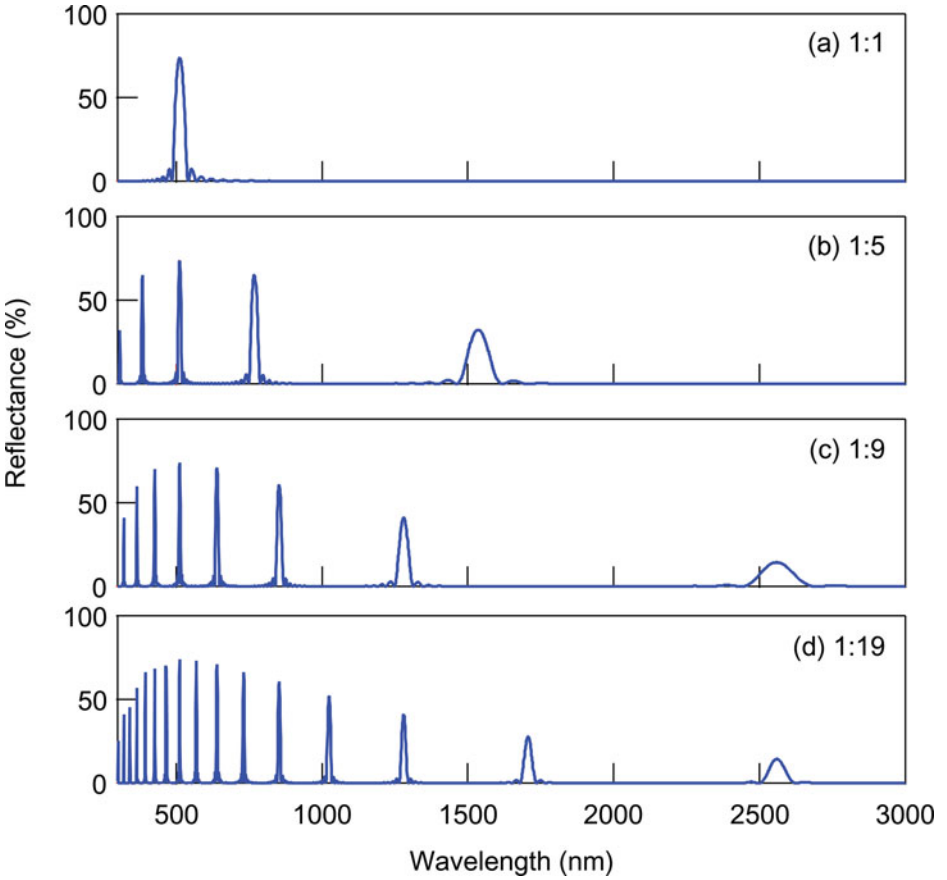

Figure 2. Calculated reflection spectra of the azo-multilayer for several optical thickness ratios of azo-layer and non-azo-layer. In these calculations, the thickness of the azo-layer is 80 nm constant, while the thickness of the non-layer increases up to 19 times of the azo-layer in optical length: (a) 85 nm, (b) 427 nm, (c) 768 nm, and (d) 1621 nm.

512 nm in Fig. 2(a). The other spectra in Fig. 2(b)-2(d) are obtained from non-quarter-wave conditions with different thick ratios. In Fig. 2, the most notable is that the number of reflection peaks increases with increasing thickness of the non-azo-layer. Although the width of the peaks is getting narrower with increasing the number of peaks, a large number of peaks appear in visible light regions. The reason of increasing the number of peaks is that the 1st mode of stopband shifts to longer wavelengths due to the increase in thickness of the non-azo-layer. That is, the peaks for shorter wavelengths indicate high order reflections. The reason is trivial, but it is very important for azobenzene because multi-stopbands are easily obtained from the multilayer having very thin azo-layers.

It is difficult to obtain a very thick layer with an accurate thickness by spin coating. To obtain non-quarter-wave multilayers, we fabricated the multilayered films by alternate spin coating of PMAz6Ac, PVA, and Poly(methyl methacrylate) (PMMA) solutions on a glass substrate. As shown in Figure 3, the alternately stacked PVA and PMMA layers are regarded as one thick-non-azo-layer. It is important that the solvent for PVA is water but PMMA is insoluble in water. In addition, the PVA and PMMA layers are almost same optically in

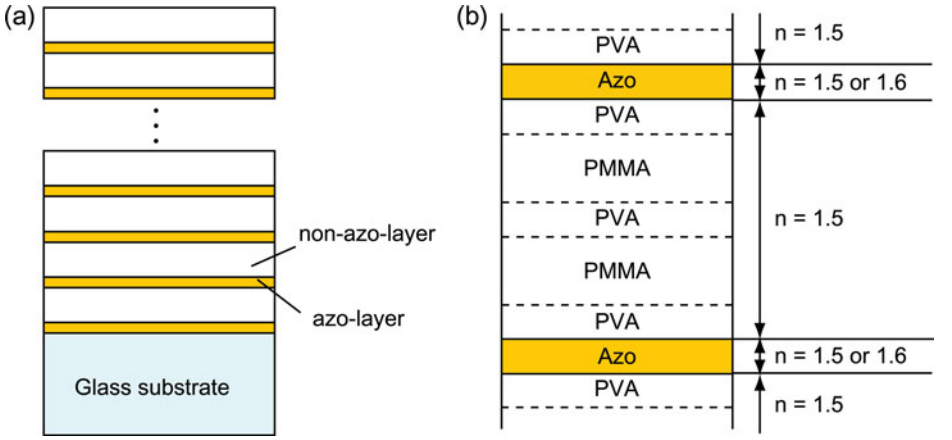

Figure 3. Configuration of the experimentally fabricated non-quarter-wavelength multilayer. The thick-non-azo-layers were obtained by stacking PVA and PMMA layers.

the viewpoint of material for a dielectric multilayer because the refractive indices of PVA and PMMA are about 1.5, and 1.49, respectively. Spin coatings were performed as follows: spin rate of 3000 rpm with 5.0 wt% of PMAz6Ac in cyclohexanone, 2.5 wt% of PVA in water, and 10.0 wt% of PMMA in toluene. After the spin coating each layer was dried for 10 min at room temperature. In the fabricated multilayer, trans-form azobenzene molecules aligned randomly because of no orientation treatment.

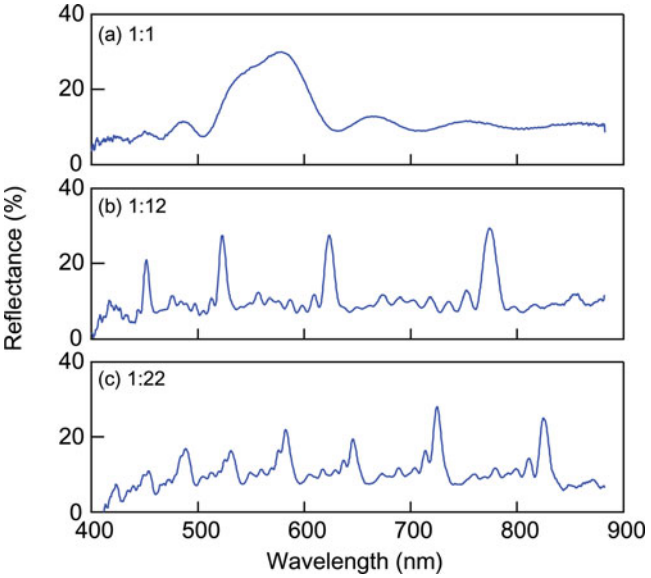

Figure 4. Reflection spectra of the azo-multilayer for several optical thickness ratios of the azo-layer and non-azo-layer: (a)1:1, (b) 1:12, and (c) 1:22.

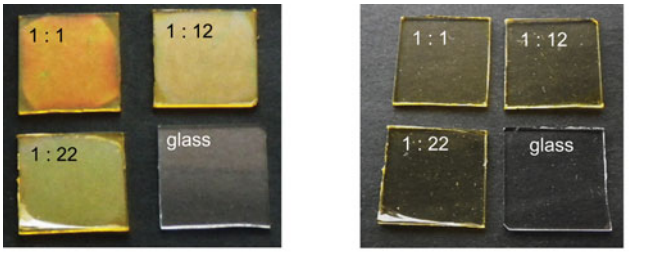

Figure 5. Photographs of the fabricated azo-multilayers in reflection and transparency states.

Fig. 4(a) shows a reflection spectrum of a quarter-wave azo-multilayer, whereas Fig. 4(b) and 4(c) show reflection spectra of non-quarter-wave azo-multilayers. All multilayers consisted of a period of 10 optical bilayers. In the non-quarter-wave multilayer, as shown in Figure 3, one optical bilayer consisted of one thin-azo-layer and one thick-non-azo-layer. As with the calculations in Figure 2, the number of peaks increases with increasing the thickness of non-azo-layer. Fig. 5(a) shows the photographs of the multilayers for the reflection state. The reflection spectrum of the multilayer with ratio of 1:1 has a single peak, and the reflection color is orange. The ratio is represented the thickness ratio between the azo-layer and non-azo-layer in optical length. In contrast, the multiple peaks appear in the reflection spectrum for the ratio of 1:12. Since the spectrum for the ratio of 1:12 has red, green, and blue peaks, the reflection color is whitish-yellow. The multilayer for the ratio of 1:22 shows more peaks, but the reflection color is pale green because the peak intensities at shorter wavelengths are weak. We consider that uniformity and accuracy of the thicknesses of spin-coated layers deteriorated in the multilayer with ratio of 1:22. On the other hand, Figure 5(b) shows the photographs of the multilayers for the transparency state after 436-nm light irradiation. It is clearly seen that the colors of all multilayers disappear.

Figure 6 shows the spectral change for the multilayer of the ratio of 1:22 by the light irradiations. Before the light irradiation, the reflection spectrum has many peaks as shown in Fig. 6(a). To control the refractive index of the azo-layers, photoirradiation was performed by using a 500 W high pressure Hg lamp with adequate cut-off filters for 436-nm light. Figure 6(b) shows the reflection spectrum of the multilayer after the 436-nm light irradiation of 320 mW/cm^2 for 30 min. The reflection peaks disappeared from the spectrum. Molecular reorientation occured during the 436-nm light irradiation, and finally we obtained homeotropic alignment. When the azobenzene molecules homeotropically align, the refractive index of azo-layer becomes 1.5 for normally incident light. In this alignment, the multilayer does not show strong reflection because PVA and PMMA also have almost the same index value. To recover the reflection peaks, we irradiated 365-nm UV light of 30 mW/cm^2 for 15 min using the Hg lamp with adequate cut-off filters. The reflection spectrum of the multilayer after the UV light irradiation is shown in Figure 6(c), in which the reflection peaks are clearly recovered.

The details of the mechanism of molecular orientation are as follows. The visible light of 436 nm is absorbed by both trans-form and cis-form. In this case, the irradiation of 436-nm light simultaneously yields trans-cis isomerization and cis-trans isomerization. The two isomerizations induce molecular motion in the azo-layers, and then molecular reorientation occurs with the photoinduced movement. However, homeotropically aligned molecules in

the azo-layers do not have such motion because the 436-nm light is not absorbed in the short molecular axis of the azobenzene molecule. Therefore, when non-polarized 436-nm light is irradiated, the photoinduced movement results in reorientation of the molecules along the unmoving homeotropically aligned molecules.

We also measured angular dependences of the reflection spectra of the non-quarter-wave multilayers. Figures 7(a) and 7(b) show the reflection spectra for the ratios of 1:12 and 1:22, respectively. The reflection peaks shift to shorter wavelengths with increasing incident angle. For the ratio of 1:22, the reflection peaks exist in visible region with a certain interval at any incident angles. This is because a reflection peak at near infrared region shifts to visible region at high incident angles. It is well known that one-dimensional multilayers have angular dependence of reflection color as an inevitable phenomenon. We consider that the non-quarter-wave multilayer having multi reflection peaks can reduce a change in reflection color. The next section discusses the details of angular dependence of reflection from the non-quarter-wave multilayer using the XYZ color space.

Angular Dependence of Reflection from Non-Quarter-Wave Multilayer

The non-quarter-wave multilayer showed many spectral peaks in a wide range of visible wavelength. Concerning angular dependence of reflection color, the multi-wavelength peak would suppress change in color. However, we cannot directly recognize the reflection color from the spectral profile. It is very difficult to judge whether color change is suppressed or not. To quantitatively discuss the color change, we tried to reproduce reflection color from the spectral profile based on CIE XYZ color space.

The color matching functions are the tristimulus values of the equal-energy spectrum as a function of wavelength [22]. These functions are intended to correspond to the sensitivity

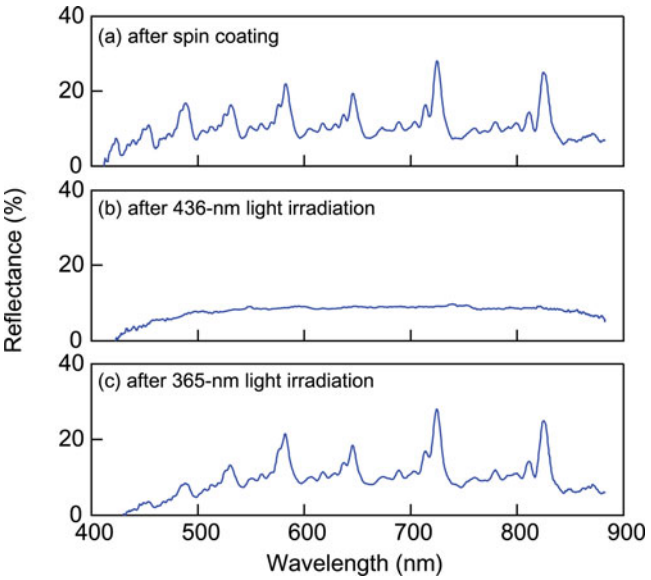

Figure 6. Reflection spectra of the fabricated non-quarter-wavelength multilayer: (a) after spin coating, (b) after the 436-nm light irradiation of 320 mW/cm^2 for 30 min, and (c) after 365-nm UV light irradiation of 30 mW/cm^2 for 15 min.

of the human eye. In particular, the $\bar{y}$color matching function includes eye's sensitivity to brightness. The XYZ tristimulus values are calculated by

$$\begin{aligned} \mathrm{X} &= \mathrm{K} \int^{\mathrm{R}} (\lambda)\, \mathrm{P}(\lambda)\, \bar{x}(\lambda)\, d\lambda \\ \mathrm{Y} &= \mathrm{K} \int^{\mathrm{R}} (\lambda)\, \mathrm{P}(\lambda)\, \bar{y}(\lambda)\, d\lambda \\ \mathrm{Z} &= \mathrm{K} \int^{\mathrm{R}} (\lambda)\, \mathrm{P}(\lambda)\, \bar{z}(\lambda)\, d\lambda \\ \mathrm{K} &= 100 \int^{\mathrm{P}} (\lambda)\, \bar{y}(\lambda)\, d\lambda \end{aligned} \tag{1}$$

where λ is wavelength, $R(\lambda)$ is the reflectance of sample, and $P(\lambda)$ is the intensity of light source. In these calculations, we used the calculated reflection spectra of a multilayer as $R(\lambda)$.

The transformation from XYZ color space to sRGB color space is given by the following matrix [23]

$$\begin{bmatrix} R_{sRGB} \\ G_{sRGB} \\ B_{sRGB} \end{bmatrix} = \begin{bmatrix} 3.2410 & -1.5374 & -0.4986 \\ -0.9692 & 1.8760 & 0.0416 \\ 0.0556 & -0.2040 & 1.0570 \end{bmatrix} \begin{bmatrix} X \\ Y \\ Z \end{bmatrix} \tag{2}$$

The gamma correction of RGB is carried out by

- i) $\mathrm{R_{sRGB}}, \mathrm{G_{sRGB}}, \mathrm{B_{sRGB}} < 0.00304$

$$\begin{aligned} \mathrm{R_{sRGB}} &= 12.92\mathrm{R_{sRGB}} \\ \mathrm{G_{sRGB}} &= 12.92\mathrm{G_{sRGB}} \\ \mathrm{B_{sRGB}} &= 12.92\mathrm{B_{sRGB}} \end{aligned} \tag{3}$$

- ii) $\mathrm{R_{sRGB}}, \mathrm{G_{sRGB}}, \mathrm{B_{sRGB}} > 0.00304$

$$\begin{aligned} \mathrm{R'_{sRGB}} &= (1.055\mathrm{R_{sRGB}})^{-\gamma} - 0.055 \\ \mathrm{G'_{sRGB}} &= (1.055\mathrm{G_{sRGB}})^{-\gamma} - 0.055 \\ \mathrm{B'_{sRGB}} &= (1.055\mathrm{B_{sRGB}})^{-\gamma} - 0.055 \end{aligned} \tag{4}$$

Finally, we obtain 8-bit RGB values for display by multiplying by 255.

$$\begin{aligned} \mathrm{R_{8bit}} &= 255\mathrm{R}, _{\mathrm{sRGB}} \\ \mathrm{G_{8bit}} &= 255\mathrm{G}, _{\mathrm{sRGB}} \\ \mathrm{B_{8bit}} &= 255\mathrm{B}, _{\mathrm{sRGB}} \end{aligned} \tag{5}$$

For accurate reproduction of the reflection color from the azo-multilayer, reproduction of the reflection spectrum of the multilayer is important. To reduce the difference between experiment and calculation, wavelength dispersions of refractive index and extinction coefficient are taken into account in calculation. Fig. 8 shows the refractive index and extinction coefficient of PMAz6Ac which measured with a thin-film thickness monitor (FE-300, Otsuka Electronics). The indices were obtained from a single layered PMAz6Ac film not a multilayered structure.

Figure 9 shows photographs and reflection spectra of the 20-bilayered films prepared by varying the concentration of PMAz6Ac in the solvent for spin coating. The multilayered films were fabricated on a glass substrate by alternate spin coating of a PMAz6Ac/cyclohexanone solution and a PVA/water solution. For the multilayered films a, b, and c in Fig. 9, the concentrations of the PMAz6Ac/cyclohexanone solutions are 3.25, 4.0, and 5.0 wt%, respectively, whereas the concentration of PVA/ water solution is 2.5wt%

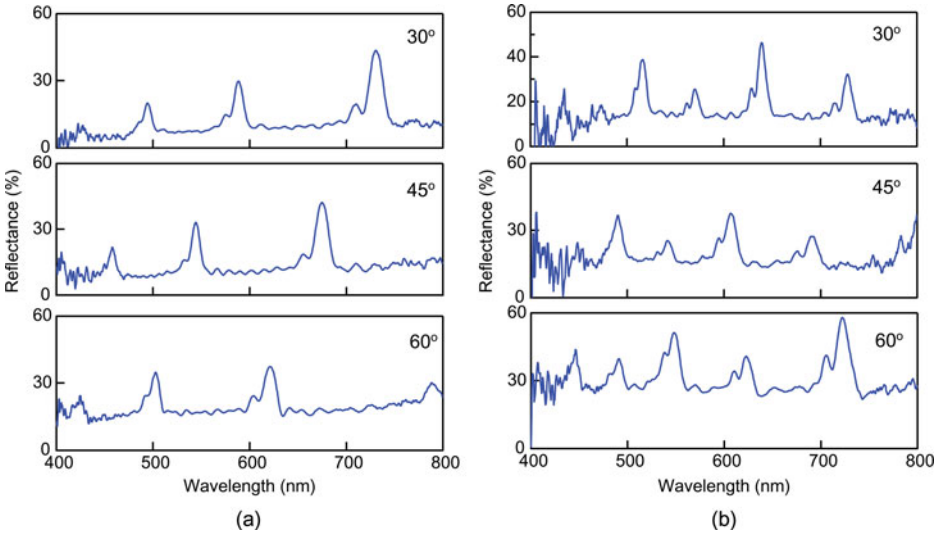

Figure 7. Angular dependences of reflection spectra of the non-quarter-wave multilayers: (a) 1:12 and (b) 1:22.

constant. The thickness of the PVA layer was 120 nm and the thicknesses of the PMAz6Ac layer in the multilayered films a, b and c were 40, 55, and 80 nm, respectively. The three multilayers exhibit reflection colors of blue, green, and red. The reflection wavelength was shifted to longer wavelength by the increase in the concentration of PMAz6Ac in the solution, indicating the increase in the layer thickness.

Figure 10 shows the calculated reflection spectra and the reproduced color images of the azo-multilayer films. The calculated green and red spectra show good agreement with experimental spectra shown in Fig. 9. The blue spectrum shows agreement of reflection wavelength, whereas the calculated reflection intensity is lower than experimental one. We suppose that the refractive index includes experimental error caused by molecular orientation. In this case, the azobenzene molecules do not aligned along a certain direction in both of the spin-coated film and the multilayer. When the azobenzene molecules align randomly in in-plane, the macroscopic refractive index becomes larger than that of 3D randomly aligned one. We consider that the molecular alignment in the PMAz6Ac thin film for refractive index measurement is tilted from the glass substrate. On the other hand, all

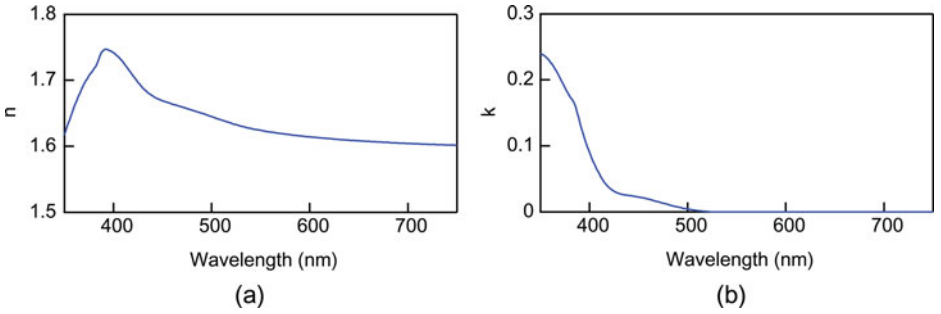

Figure 8. Wavelength dispersions of (a) refractive index and (b) extinction coefficient of PMAz6Ac.

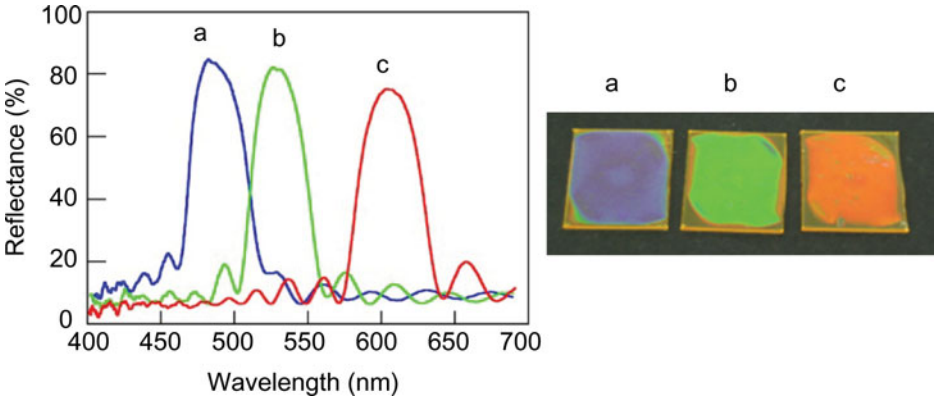

Figure 9. Photographs and reflection spectra of multilayered films prepared by alternative spin coating of 2.5 wt% PVA/water and (a) 3.25, (b) 4.0, and (c) 5.0 wt% PMAz6Ac/cyclohexanone.

reproduced color images of the azo-multilayer looks similar to the fabricated multilayered films. These results indicate that this calculation method is quite useful to investigate the reflection color from multilayered structures.

Let us discuss the angular dependence of reflection color from quarter-wave and non-quarter-wave multilayers. To compare two multilayers, we calculated the reflection colors using 4×4 matrix method as a function of incident angle. We assumed that the quarter-wave multilayer consisted of 100-nm non-azo-layer and 93-nm azo-layer. Fig. 11(a) shows the reflection spectra from the quarter-wave multilayer for various incident angles. In these calculations, the number of the multilayer period was 20 and the polarization of incident light was set to be linear with angle of 45°. The reflection peak appeared at 600 nm for normal incidence, and then the reflection peak was blue shifted to 500 nm with increasing incident angle. That is, roughly speaking, the reflection color changed from orange to blue-green. To understand the color change in quantitative way, we ploted the reflection colors in the *xy* color space. Fig. 11(b) show the angular dependence of the reflection color in the

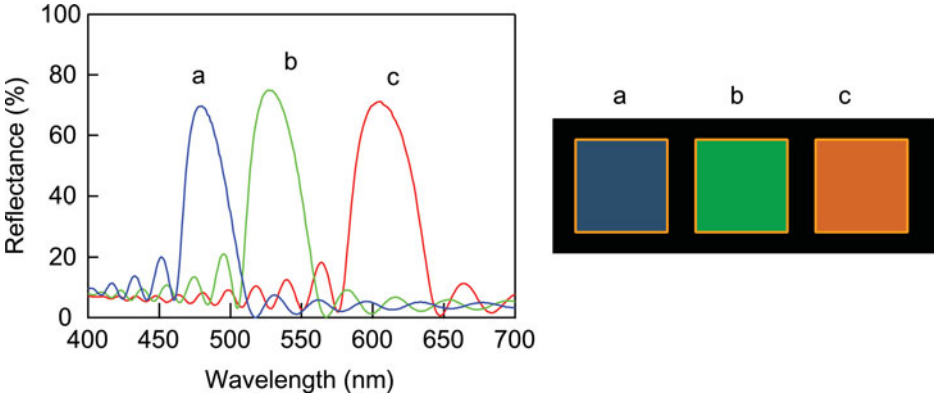

Figure 10. Reproduced color images and calculated reflection spectra of multilayered films. The thickness of PVA layers is constant 120 nm. The thickness of azo-layer are (a) 39 nm, (b) 54 nm, and (c) 78 nm, respectively.

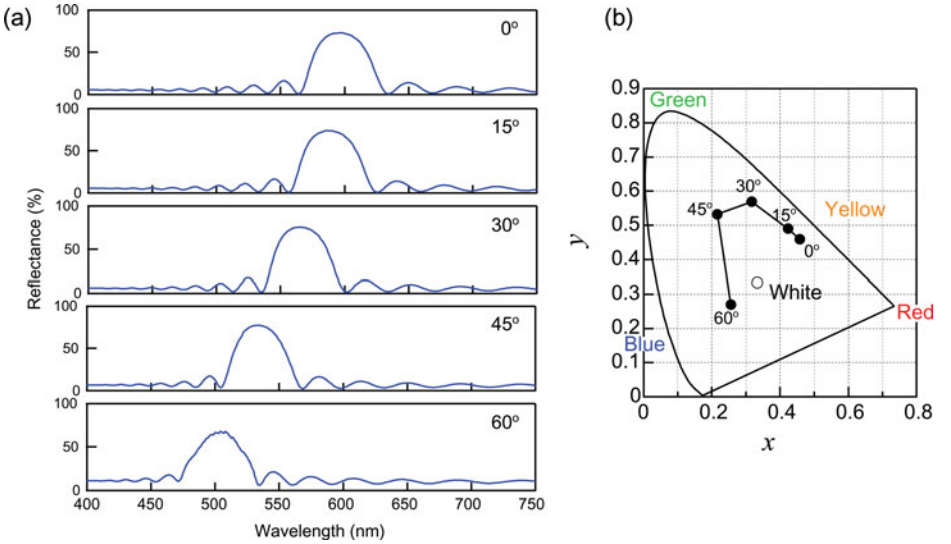

Figure 11. (a) Calculated reflection spectra from the quarter-wave multilayer for 0°, 15°, 30°, 45°, and 60° incident angles. (b) Angular dependence of *xy* value obtained from the reflection color of the multilayer.

xy space. Here the filled circles represent reflection color and the open circle is the white point. The *xy* values are obtained by

$$\begin{aligned} \mathrm{x} &= \mathrm{X}/(\mathrm{X}+\mathrm{Y}+\mathrm{Z}) \\ \mathrm{y} &= Y/(\mathrm{X}+\mathrm{Y}+\mathrm{Z}) \end{aligned} \tag{6}$$

where X, Y, and Z are tristimulus values calculated using Equation 1. It is obvious that the reflection color moves from yellow region to blue region with increasing incident angle. On the other hand, the angular dependence of the reflection for non-quarter-wave multilayer is shown in Fig. 12. The reflection spectra from the quarter-wave multilayer for various incident angles are shown in Fig. 12(a). In these calculations, we assumed that the non-quarter-wave multilayer consisted of 1500-nm non-azo-layer and 60-nm azo-layer. Other conditions for the calculation were the same in the case of the quarter-wave multilayer. At incident angle of 0°, there were five peaks in the range 400 to 700 nm. Each peak shifted to shorter wavelength with increasing incident angle. This behavior is the same as the peak of the quarter-wave multilayer. However, in the case of the non-quarter-wave multilayer, additional peak enter the visible region from near infrared region. For example, new peak appears at 735 nm for incident angle of 30°. This additional peak suppresses the change in color with increasing incident angle. Fig. 12(b) shows the angular dependence of *xy* color value for the non-quarter-wave multilayer. Note that all reflection colors are plotted near the white point. This indicates that the angular dependence of reflection color for the non-quarter-wave multilayer is small compared with conventional quarter-wave multilayer.

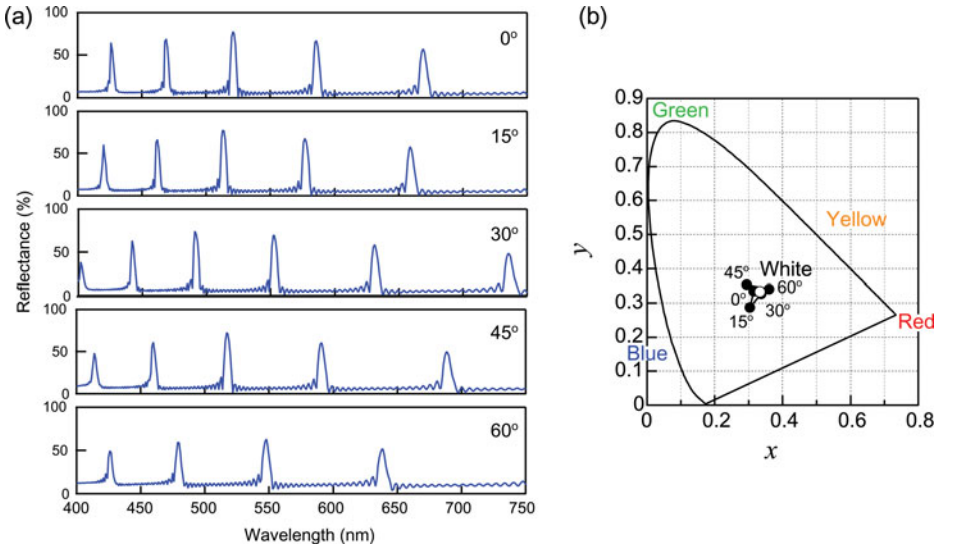

Figure 12. (a) Calculated reflection spectra from the non-quarter-wave multilayer for 0°, 15°, 30°, 45°, and 60° incident angles. (b) Angular dependence of *xy* value obtained from the reflection color of the multilayer.

Conclusion

The reflection properties of the non-quarter-wave multilayered structure including thin azobenzene layers were studied experimentally and numerically. We fabricated the non-quarter-wave multilayers by alternate spin coating of PMAz6Ac, PVA, and PMMA solutions on a glass substrate. The non-quarter-wave multilayers having thin PMAz6Ac layers exhibited multi-peak reflection in visible regions. To quantitatively investigate the angular dependence of the reflection color, the reflection spectra were calculated by using the 4 × 4 materix method, and then the spectral color reproductions were carried out. In a conventional quarter-wave multilayer, the reflection color moved from yellow region to blue region with increasing incident angle. In contrast, the reflection colors from incident angle 0° to 60° appeared near the white point in *xy* color space. This indicates that the angular dependence of reflection color was small compared with conventional quarter-wave multilayer. We believe that the study will contribute to a better knowledge of optically switchable multilayer using azobenzene polymers.

Funding

This work was supported by JSPS KAKENHI Grant Numbers 23350115 and 25790042, and the Core Research for Evolutional Science and Technology (CREST) of the Japan Science and Technology Agency (JST).

References

[1] Ikeda, T., Horiuchi, S., Karanjit, D. B., Kurihara, S., & Tazuke, S. (1990) *Macromolecules*, *23*, 42.
[2] Ikeda, T. & Tsutsumi, O. (1995) *Science*, *268*, 1873.

[3] Kubo, S., Gu, Z. Z., Takahashi, K., Ohko, Y., Sato, O., & Fujishima, A. (2002) *J. Am. Chem. Soc.*, *124*, 10950.
[4] Kurihara, S., Moritsugu, M., Kubo, S., Kim, S.N., Ogata, T., Nonaka, T., & Sato, O., (2007) *European Polymer Journal*, *43*, 4951.
[5] Moritsugu M., Ishikawa, T., Kawata, T., Ogata, T., Kuawahara, Y., & Kurihara, S. (2011) *Macromolecular Rapid Communications*, *32*, 1546.
[6] Ujiie, S. & Iimura, K. (1992) *Macromolecules*, *25*, 3174.
[7] Date, R. W., Fawcett, A. H., Geue, T., Haferkorn, J., Malcolm, R. K., & Stumpe, J. (1998) *Macromolecules*, *31*, 4935.
[8] Sapich, B., Vix, A. B. E., Rabe, J. P., Stumpe, J., Wilbert, G., & Zentel, R. (2006) *Thin Solid Films*, *514*, 165.
[9] Rais, D., Zakrevskyy, Y., Stumpe, J., Nespurek, S., & Sedlakova, Z. (2008) *Opt. Mater.*, *30*, 1335.
[10] Wielen, M. W. J. van der, Cohen Stuart, M. A., Fleer, G. J., Boer, D. K. G. de, Leenaers, A. J. G., Nieuwhof, R. P., Marcelis, A. T. M., & Sudholter, E. J. R. (1997) *Langmuir*,*13*, 4762.
[11] Wong, G. C. L., Commandeur, J., Fischer, H., & Jeu, W. H. de, (1996) *Phys. Rev. Lett.*, *77*, 5221.
[12] Tian, Y., Watanabe, K., Kong, X., Abe, J., & Iyoda, T. (2002) *Macromolecules*, *35*, 3739.
[13] Bobrovsky, A., Boiko, N., Shibaev, & V., Stumpe, J., (2004) *J. Photochem. Photobiol. A: Chem.*, *163*, 347.
[14] Yoshino, K., Shimoda, Y., Kawagishi, Y., Nakayama, K., & Ozaki, M. (1999) *Appl. Phys. Lett.*, *75*, 932.
[15] Leonard, S. W., Mondia, J. P., Driel, H. M. van, Toader, O., John, S., Busch, K., Birner, A., Gösele, U., & Lehmann, V. (2000) *Phys. Rev. B*, *61*, R2389.
[16] Ozaki, R., Shinpo, T., Yoshino, K., Ozaki, M., & Moritake, H. (2008) *Appl. Phys. Express*, *1*, 012003.
[17] Clark, J. & Lanzani, G. (2010) *Nature Photonics*, *4*, 438.
[18] Kimura, M., Okahara, K., & Miyamoto, T. (1979) *J. Appl. Phys.*, *50*, 1222.
[19] Komikado, T., Yoshida, S., & Umegaki, S. (2006). *Appl. Phys. Lett,. 89*, 061123.
[20] Kurihara, S., Moritsugu, M., Kubo, S., Kim, S., Ogata, T., Nonaka, T., & Sato, O. (2007) *Eur. Polym. J.*, *43*, 4951.
[21] Berreman, DW. (1973). *J. Opt. Soc. Am.*, *63*, 1374.
[22] CVRL Color & Vision Database, http://www.cvrl.org/.
[23] Stokes, M., Anderson, M., Chandrasekar, S., & Motta, R. (1996) A standard default color space for the internet - sRGB, http://www.color.org/sRGB.html.